Dalton Transactions

Accepted Manuscript

This article can be cited before page numbers have been issued, to do this please use: L. Tei, Z. Baranyai, L. Gaino, A. Forgacs, A. Vagner and M. Botta, *Dalton Trans.*, 2015, DOI: 10.1039/C4DT03939D.

ROYAL SOCIETY OF CHEMISTRY

www.rsc.org/dalton

Cite this: DOI: 10.1039/c0xx00000x

www.rsc.org/xxxxxx

ARTICLE TYPE

Thermodynamic stability, kinetic inertness and relaxometric properties of monoamide derivatives of lanthanide(III) DOTA complexes

Lorenzo Tei,[a] Zsolt Baranyai,[b] Luca Gaino,[a] Attila Forgács,[a] Adrienn Vágner [b] and Mauro Botta*[a]

Received (in XXX, XXX) Xth XXXXXXXXX 20XX, Accepted Xth XXXXXXXXX 20XX
DOI: 10.1039/b000000x

A complete thermodynamic and kinetic solution study on lanthanide(III) complexes with monoacetamide (DOTAMA, **L1**) and monopropionamide (DOTAMAP, **L2**) derivatives of DOTA (DOTA = 1,4,7,10-tetraazacyclododecane-1,4,7,10-tetraacetic acid) was undertaken with the aim to elucidate their stability and inertness in aqueous media. The stability constants of Gd**L1** and Gd**L2** are comparable, whereas a more marked difference is found in the kinetic inertness of the two complexes. The formation of the Eu(III) and Ce(III) complexes takes place via the formation of the protonated intermediates which can deprotonate and transform into the final complex through a OH^- assisted pathway. Gd**L2** shows faster rates of acid catalysed decomplexation with respect to Gd**L1**, which has a kinetic inertness comparable to GdDOTA. Nevertheless, Gd**L2** is one order of magnitude more inert than GdDO3A. A novel DOTAMAP-based bifunctional chelating ligand and its deoxycholic acid derivative (**L5**) were also synthesized. Since the coordinated water molecule in Gd**L2** is characterized by an exchange rate ca. two order of magnitude greater than in Gd**L1**, the relaxivity of the macromolecular derivatives of Gd**L5** should not be limited by the slow water exchange process. The relaxometric properties of the supramolecular adduct of Gd**L5** with Human Serum Albumin (HSA) were investigated in aqueous solution by measuring the magnetic field dependence of the ^1H relaxivity that, at 20 MHz and 298 K, shows a 430% increase over that of the unbound Gd**L5** chelate. Thus, Gd(III) complexes with DOTAMAP macrocyclic ligands can represent good candidates for the development of stable and highly effective bioconjugate systems for molecular imaging applications.

Introduction

Magnetic Resonance Imaging (MRI) has rapidly gained a position of prominence in diagnostic clinical medicine and biomedical research due to numerous favourable features: non-invasiveness, great spatial and temporal resolution, deep tissue penetration, excellent inherent soft tissue contrast, easy access to the detailed anatomical and functional information. The intrinsic contrast is further improved by the use of contrast agents (CAs) both in the clinical setting and in the preclinical research laboratories. The use of CAs allows adding further physiological information of great importance to the excellent anatomical resolution typically observed in the images acquired in MRI. Furthermore, CAs enable to decrease the time for image acquisition, improve the reliability of the diagnosis and reduce artefacts. Over the past two decades, the extensive utilization of Gd(III) complexes as MRI T_1 shortening agents has also had a profound influence on the research in the field of lanthanide coordination chemistry. In fact, a primary goal in the development of Gd-based CAs is the improvement of the efficiency of the probes through optimization of the molecular parameters that control the magnetic coupling between the paramagnetic ion and water molecules. The efficiency is typically measured by the longitudinal proton relaxivity (r_1, the increase in the water proton relaxation rate per mM concentration of Gd) that, for the clinically approved Gd(III) complexes, lies in the range 4−5 mM^{-1} s^{-1}, at 20 MHz (0.47 T) and 298 K.[1] The key molecular parameters that govern the relaxivity of a Gd(III) complex, according to the established theory of paramagnetic relaxation, are the number (q) and residence lifetime, τ_M, of the inner sphere water molecule(s) and the rotational motion of the paramagnetic system, described by the correlation time τ_R.[1]

Another fundamental issue in the development of CAs, increasingly important in recent years, is related to the stability of the MRI probes with respect to the potential release of toxic gadolinium ions *in vivo*. It has been long recognized that, for a safe *in vivo* use, Gd(III) ion needs be encapsulated into a chelate characterized by high thermodynamic stability and kinetic inertness.[2] This is typically achieved with octadentate polyaminocarboxylate chelators mainly based on two structural motifs: the macrocyclic 1,4,7,10-tetraazacyclododecane-1,4,7,10-tetraacetic acid (DOTA) and the acyclic diethylenetriamine pentaacetic acid (DTPA). In particular, high *in vivo* stability is required when the probe is used for targeting procedures or in other cases that involve a slow excretion (*i.e.* impaired kidney function) so that the longer residence time is associated with a greater risk of dissociation. In fact, it has been recently reported that the release of Gd(III) ions from MRI probes based on acyclic ligands in patients with renal failure is related to the occurrence of Nephrogenic Systemic Fibrosis (NSF), a very rare but severe

View Article Online
DOI: 10.1039/C4DT03939D

disease.[3-6] Metal ion dissociation was not observed with macrocyclic chelates and several studies both *in vitro* and *in vivo*, in mice and in humans, consistently demonstrated that kinetic inertness of macrocyclic Gd(III) complexes is superior to that of acyclic ones.[5-10] Based on these results, Gd-chelates with derivatives of DOTA are considered the most kinetically inert and are therefore most suitable for *in vivo* applications. A class of compounds of particular importance is represented by the DOTA monoamide derivatives that allow obtaining complexes kinetically inert and electrically neutral. Since an initial report on the high values of the formation constant,[11] a large number of DOTA monoamide derivatives have been synthesized and characterized for stable complexation of lanthanide cations.[1, 12-16] Typically, GdDOTA-like chelates present only one inner sphere water molecule (q = 1) and their relaxivity can be enhanced by increasing the molecular size, *i.e.* by conjugating the paramagnetic complexes to a variety of macromolecular substrates, and, hence, by slowing down the rotational tumbling rate ($1/\tau_R$). For example, the reversible formation of host-guest adducts between suitably functionalized Gd(III) complexes and human serum albumin (HSA) represents one of the first strategies used to achieve large relaxation enhancements.[17] However, it has been understood earlier that if the water exchange rate (k_{ex} = $1/\tau_M$) is not sufficiently fast ($\geq 5 \times 10^7$ s^{-1}) the expected increase of r_1 for Gd-based macromolecular systems is severely limited.[18] To highlight the key role of a short τ_M, we have recently reported a preliminary study which compares the relaxometric behavior of two GdDOTA monoamide complexes (Gd**L1** and Gd**L2** in Scheme 1) and of the micellar aggregates formed by their amphiphilic derivatives bearing a stearoyl chain.[19] In particular, we have shown that increasing the length of the carboxyamide arm from acetic (DOTA-monoacetamide = DOTAMA) to propionic (DOTA-monopropionamide = DOTAMAP) accelerates k_{ex} by nearly two orders of magnitude. In turn, this translates into r_1 enhancements of the lipid aggregates, at 0.47 T, from +130% at 278 K to +22% at 310 K. Such an increase in k_{ex} for GdDOTAMAP was attributed to a greater steric compression at the water coordination site, which induces an acceleration of the dissociatively activated exchange process, in agreement with previous findings of Éva Tóth and coworkers.[20] Similar results for DOTA monopropionate derivatives, structurally related but featuring a net negative charge, have been recently reported.[21-23] Since the substitution of an acetamide by a propionamide might be accompanied by an undesired decrease of the thermodynamic stability and of the kinetic inertness, a complete thermodynamic and kinetic solution study on lanthanide complexes with the two ligands has been undertaken. In the previous work only the stability constants of Gd**L1** and Gd**L2** (log$K$ = 20.86 and 20.22, respectively) were measured.[13] Curiously enough, although DOTAMA-like ligands have been widely used in the literature, only a very limited number of thermodynamic solution date have been reported[24, 25] and no kinetic studies have been published so far. Moreover, in order to highlight further the efficacy of the GdDOTAMAP-like chelates to enhance r_1 of macromolecular probes, a novel DOTAMAP-based bifunctional chelating ligand and its deoxycholic acid derivative (**L5**) were synthesized.

This targeting synthon has a strong affinity for HSA and has been used in the literature conjugated to Gd-chelates as hepatospecific or Dynamic Contrast Enhanced (DCE) MRI contrast agents.[26, 27] For instance, a DTPA-like contrast agent showing high biliary excretion and a great potential for hepatobiliary imaging was reported some years ago.[28] Finally, the relaxometric properties of Gd**L5** and its supramolecular adduct with HSA were investigated in aqueous solution by measuring the magnetic field dependence of the ^{1}H relaxivity.

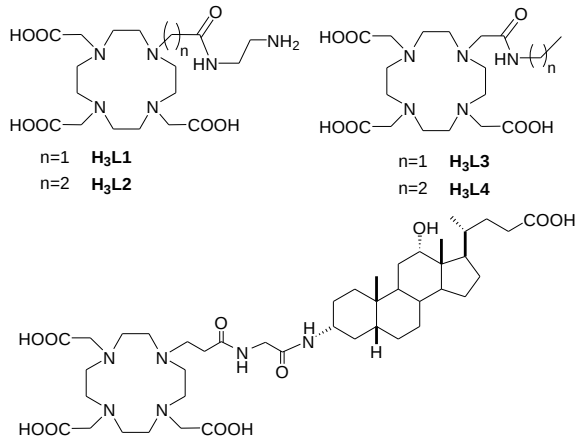

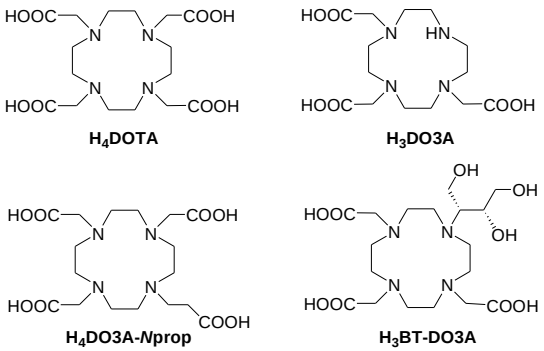

Scheme 1. The structure of the ligands discussed in the text.

Results and Discussion

Solution equilibrium studies.

The replacement of one negatively charged carboxylate group of DOTA with a neutral amide group is known to significantly reduce the overall affinity of the ligand for the Ln^{3+}-ions. Hence, the stability constants (logK_{LnL}) of LnDOTA-monoamide complexes are typically 3 - 4 orders of magnitude lower than those of the LnDOTA-like complexes. A comparison of logK_{GdL} values between Gd**L1** and Gd**L2** was reported in a preliminary communication; here, we present the results of a more detailed and thorough investigation on the solution properties of the Ln(III) complexes of L1 and L2 in order to clarify the effects of the increased length of the amide pendant arm on the equilibrium properties of the Ln(III)-complexes.

Protonation equilibria: The protonation constants of H_3**L1** and H_3**L2** (logK_i^H, i = 1, 2…6), defined by Equation (1), were determined by pH-potentiometry and are listed in Table 1 where are compared with those of H_4DOTA, H_3DO3A, and two H_3DOTA-monoamide ligands (**L3** and **L4**).

View Article Online
DOI: 10.1039/C4DT03939D

$$K_i^H = \frac{[H_iL]}{[H_{i-1}L][H^+]} \quad (1)$$

The protonation scheme of DOTA-like ligands is well known and it has been fully characterized with both spectroscopic and potentiometric methods.[29-31] Thus, we may safely assume that the first and second protonation processes occur at two opposite ring nitrogen atoms, whereas the third and fourth protonation steps take place at the carboxylate groups of the acetic arms attached to the non-protonated ring nitrogen atoms, because of the greater charge separation and lower electrostatic repulsion between the protonated donor atoms.[29]

Table 1. Protonation constants of H_3**L1**, H_3**L2**, H_3DOTAMA-ethyl (H_3**L3**) and H_3DOTAMA-propyl (H_3**L4**), H_3DO3A and H_4DOTA (0.1 M KCl, 298K). Standard deviations are shown in parentheses.

	H_3**L1**	H_3**L2**	H_3**L3**[a]	H_3**L4**[b]	H_3**DO3A**[c]	H_4**DOTA**[c]
logK_1^H	11.77(2)	11.00 (3)	9.6	10.17	11.99	11.41
logK_2^H	9.98 (1)	9.52 (2)	9.2	9.02	9.51	9.83
logK_3^H	9.33 (1)	8.98 (4)	4.4	4.41	4.30	4.38
logK_4^H	4.01 (1)	4.59 (5)	1.7	2.94	3.63	4.63
logK_5^H	1.99 (1)	3.12 (5)	–	1.99	1.84	1.92
logK_6^H	1.53 (3)	1.88 (5)	–	–	–	1.58
$\sum_{i=1}^{4} \log K_i^H$	35.09	34.09	24.9	26.54	29.43	30.25

[a] Ref. [24] in NaCl (0.1 M), [b] Ref. [25] in KCl (1.0 M), [c] Ref. [30] in KCl (0.1 M)

A comparison of protonation constants of **L1** and **L2** with those of DOTA and DO3A (Table 1) indicates that logK_1^H and logK_2^H values are substantially comparable, whereas the logK_3^H values for **L1** and **L2** are nearly five orders of magnitude higher than for DOTA and DO3A. By considering the protonation constants of *β*-alaninamide (logK_1^H=9.32),[32] we can make the reasonable assumption that the third protonation for **L1** and **L2** involves the nitrogen atom of the pendant amino group. Finally, logK_4^H, logK_5^H and logK_6^H, corresponding to the protonation of three carboxylate groups, have similar values to those of DO3A and DOTA. It is worth noting that the logK_1^H value of **L1** and **L2** is higher than that of the two DOTA-monoamide ligands, **L3** and **L4**. A possible explanation concerns the different ionic strength used in the equilibrium studies of **L3** and **L4** (Table 1): the formation of weak Na^+- and K^+-complexes competing with the first protonation process may be responsible of the lower value of the protonation constant. Similar effects were observed for a number of DOTA and DO3A derivatives.[33]

The total basicity ($\sum_{i=1}^{4} \log K_i^H$) of **L1** and **L2** is higher than that of DOTA and DO3A because of the relatively high protonation constant of the terminal amine nitrogen atom (Table 1). However, not considering the logK^H value for the protonation of the terminal amino group, we obtain the $\sum_{i=1}^{4} \log K_i^H$ values of 27.75 and 28.23 for **L1** and **L2**, respectively. These values are significantly lower than for DOTA and comparable to that of DO3A. It follows that the thermodynamic stability of the lanthanide(III) complexes of **L1** and **L2** should be lower than that for the DOTA complexes and comparable to the DO3A complexes. Since the coordination of the amide oxygen of **L1** and **L2** to the metal ion results in the formation of five- and six-membered chelate rings, respectively, significant differences in their interaction with Ln^{3+} ions are expected.

Complexation properties: Often, the complex formation equilibria between macrocyclic ligands and Ln^{3+} ions cannot be studied by direct pH potentiometric titration because of the slow formation kinetics.[34-42] Thus, the stability and protonation constants of Ln**L1**, Gd**L2** and LnDO3A complexes, defined by Eqn. (2) and (3), were investigated by pH-potentiometriy and by UV-spectrophotometry (Ce^{3+} - **L1** system) using the "out of cell" procedure (298K, 0.1 M KCl) (Table 2). The UV-absorption spectra of the Ce^{3+} - **L1** system used for the calculation of logK_{CeL} value are reported in Figure S1.

$$K_{ML} = \frac{[ML]}{[M][L]} \quad (2)$$

$$K_{MH_iL} = \frac{[MH_iL]}{[MH_{i-1}L][H^+]} \quad i=1,2 \quad (3)$$

Table 2. Stability (logK_{LnL}) and protonation constants (logK_{LnHiL}) of Ln**L1**, Gd**L2**, Ln**L3** and Ln**L4**, LnDO3A and LnDOTA complexes (0.1 M KCl, 298K)

	H_3**L1**	H_3**L2**	H_3**L3**[a]	H_3**L4**[b]	H_3**DO3A**[c]	H_4**DOTA**[e]
LaL	**20.49 (8)**	–	–	–	**18.63**	**21.7**
LaHL	9.10 (4)	–	–	–	–	–
CeL	**21.24 (5)**	–	–	**19.26**	**19.7**[d]	**23.39**
CeHL	8.84 (7)	–	–	2.65	–	–
GdL	**22.25 (4)**	**20.22 (3)**	**20.1**	**21.29**	**21.56**	**24.7, 25.3**[f]
GdHL	9.24 (2)	8.40 (6)	–	2.57	–	–
LuL	**21.95 (7)**	–	–	**21.83**	**21.44**	**25.4**
LuHL	8.90 (4)	–	–	2.33	–	–

[a] Ref. [24] in NaCl (0.1 M), [b] Ref. [25] in KCl (1.0 M), [c] Ref. [30] in KCl (0.1 M) [d] Ref. [43] in $(Me)_4NCl$ (0.1 M), [e] Ref. [44] in NaCl (0.1 M), [f] Ref. [45] in $(Me)_4NCl$ (0.1 M).

As previously observed for the LnDO3A and LnDOTA complexes, the stability constants of Ln**L1** chelates increase moving from La(III) to Gd(III), while remaining almost constant for the heavier members of the series (Table 2).[2] The stability constants of the Ln**L1** complexes (Ln = La, Ce, Gd, Lu) are higher than those for the corresponding LnDO3A complexes and lower than those of the LnDOTA chelates, indicating not only that the amide group is involved in the coordination of the Ln(III) ions but also that it is a weaker donor than the carboxylate group. Interestingly, the stability constants for the Ln**L1** complexes are sensibly higher than those of the related DOTA monoamide derivatives Ln**L3** (Ln = Gd) and Ln**L4** (Ln = Ce, Gd, Lu). Such an effect is necessarily related to the presence of the terminal amino group and results in a stabilization particularly pronounced for the early members of the lanthanide series. The smaller value of the stability constant of Gd**L2** than for Gd**L1** and GdDO3A may be accounted for by both the lower value of the first protonation constant of **L2** and by the weaker interaction between the amide O-atom and Gd^{3+} ion associated with the formation of a less stable six-membered chelate ring. However, it should be noted that the thermodynamic stability of Gd**L2** is quite comparable to Gd**L3** and Gd**L4**, featuring an acetamide arm. Therefore, it can be concluded that the introduction of a propionamide group in place of an acetamide group in DOTA-monoamide ligands has a pronounced effect on the kinetics of

View Article Online
DOI: 10.1039/C4DT03939D

water exchange of the corresponding Gd(III) complexes without clearly affecting their stability. The stability constant of Gd**L1** differs slightly from the value previously reported ($\log K_{Gd\mathbf{L1}}$=20.86)[19] as a result of a new, more accurate determination. Finally, the protonation constants of the amino group in the Ln**L1** and Gd**L2** complexes (Table 2) are comparable with the third protonation constant of the free ligands ($\log K_3^H$), as expected for a pendant moiety not involved in the coordination of the lanthanide(III) cation.

Complex formation kinetics

The complex formation reactions **L1** and **L2** with Ln(III) ions were found to be slow in the pH range 3.5 – 6.5 where the protonated Ln(H**L1**) and Ln(H**L2**) species are predominant (Figure S2). It is well recognized that the formation reaction of macrocyclic Ln(III) complexes is generally slow,[30, 34, 40, 41, 43, 46] as a result of both the difficult encapsulation of the Ln^{3+} ions in the rigid and preformed coordination cage of DOTA-like ligands and the formation of stable protonated intermediates (*Ln(H_xL)). The formation and structure of the intermediates were investigated by spectrophotometry,[34, 37] ^{1}H-NMR[38] and luminescence spectroscopies.[35, 36] The luminescence lifetime determination of the diprotonated intermediate *Eu(H_2DOTA) indicates the presence of four or five H_2O molecules in the inner coordination sphere of the metal ion, suggesting an out-of-cage coordination of Eu(III) by four carboxylate groups and the occurrence of two protonated diametrically opposed nitrogen atoms in the tetraaza cycle.[35, 36] According to detailed kinetic studies,[34-37, 39-41] the complexation process proceeds through two steps, the first of which involves the rapid formation of the diprotonated intermediate *Ln(H_2DOTA) which is in equilibrium with the monoprotonated species *Ln(HDOTA). In the second rate-determining step, the slow and OH^- assisted deprotonation takes place, followed by the displacement of the metal ion into the cavity and rearrangement to the final complex LnDOTA.

The rates of the formation reactions of Ce(III)- and Eu(III)-complexes with **L1** and **L2** were studied by spectrophotometry in the presence of 5 - 40 folds excess of the Ln^{3+} ion in the pH range 3.5 - 6.0. The absorption spectra of the Ce^{3+}-**L1**, Eu^{3+}-**L1**, Ce^{3+}-**L2** and Eu^{3+}-**L2** reacting systems as a function of time are reported in Figures S3 and S4. From the kinetic data we obtain the pseudo first-order constants k_{obs} that, plotted as a function of the Ln(III) concentration, yield saturation curves indicating the fast formation of reaction intermediates (Figures S5 and S6). The first reaction step can be accounted for by the rapid formation of a tri-protonated intermediate (*Ln(H_3L)) in which three carboxylate groups are coordinated to the Ln^{3+} ion and two opposite tertiary nitrogen atoms of the macrocycle and the amino group are protonated. The rate-determining step of the formation of the Ln(H**L1**) and Ln(H**L2**) species is the deprotonation of a ring nitrogen atom of the *Ln(H_2**L1**) and *Ln(H_2**L2**) intermediates and the rearrangement to the final complexes. The proposed mechanism for the formation of Ln(H**L1**) and Ln(H**L2**) is reported in Scheme 2. The definitions and equations used for the evaluation of the kinetic data are reported in the Supporting Information.

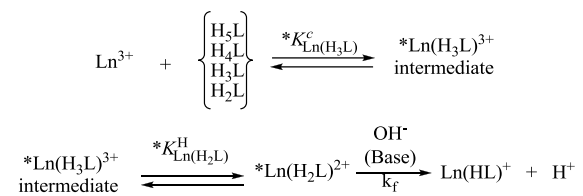

Scheme 2. The suggested pathway for the formation of Ln(H**L1**) and Ln(H**L2**).

In Scheme 2, $^*K^c_{Ln(H_3L)}$, $^*K^H_{Ln(H_2L)}$, and k_f are the conditional stability constants of *Ln(H_3**L1-2**), the protonation constant of *Ln(H_2**L1-2**) and the rate constant characterizing the deprotonation and structural rearrangement of the intermediates to the Ln(H**L1**) and Ln(H**L2**) complexes. The calculated $^*K^c_{Ln(H_3L)}$ values of *Ce(H_3L) and *Eu(H_3L) are 3.24(2) and 3.15(2) for **L1** and 2.80(2) and 2.98(4) for **L2**, respectively. These values are comparable with the conditional stability constant of the diprotonated *Gd(H_2DO3A) intermediate (3.48)[39] and lower than those reported for the *Ln(H_2DOTA) and *Ln(H_2DO3A-*N*prop) intermediates (*Ce(H_2DOTA): 4.4, *Eu(H_2DOTA): 4.3; *Ce(H_2DO3A-*N*prop): 4.51, *Gd(H_2DO3A-*N*prop): 4.50).[34, 46] According to the $^*K^c_{Ln(H_3L)}$ values obtained, one can reasonably assume that the coordination sphere in *Ln(H_3**L1**) and *Ln(H_3**L2**) is similar to that of *Ln(H_2DO3A). Moreover, the slightly higher conditional stability constants of *Ln(H_3**L1**) as compared to *Ln(H_3**L2**) may be explained by the stronger coordination of the acetamide O-atom of **L1**. The rate constants k_f for the formation of CeL and EuL (L = **L1** and **L2**) as a function of the OH^- concentration are shown in Figure 1. All k_f rate constants show a first-order dependence on [OH^-], expressed by Eq. (4),

$$k_f = k_{OH} \times [OH^-] \qquad (4)$$

that is typical for the formation LnDOTA-like complexes, where k_{OH} characterizes the OH^- assisted deprotonation of the protonated intermediates and the rearrangement to the final product.[34-39, 41]

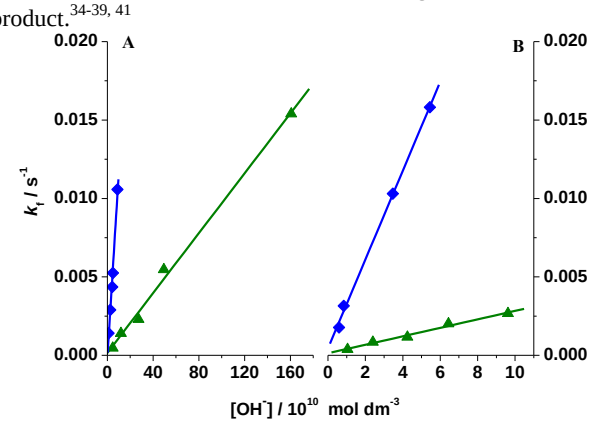

Figure 1. The k_f rate constants for the formation reactions of the Ln(H**L1**) (**A**) and Ln(H**L2**) (**B**) complexes of Ce(III) (green triangle) and Eu(III) (blue diamond) as a function of [OH^-] (0.1 M KCl, 298K).

The k_{OH} rate constants were calculated by fitting the k_f values (Figure 1) to Eqn. (4) (Tables 3). For **L1** and **L2**, these values are comparable with those of LnDOTA and LnDO3A which indicates that the replacement of a carboxylic group with a carboxyamide does not alter the formation rate of the Ln(III) complexes.

View Article Online
DOI: 10.1039/C4DT03939D

Table 3. The k_{OH} ($M^{-1}s^{-1}$) rate constants characterizing the formation of **L1**, **L2**, DOTA, DO3A-*N*prop, BT-DO3A and DO3A complexes with Ce(III) and Eu(III) (0.1 M KCl, 298K).

	$L1^{3-}$	$L2^{3-}$	$DOTA^{4-}$ [a]	DO3A-Nprop[b]	BT-DO3A[c]	$DO3A^{3-}$ [d]
Ce(III) ($\times10^{-5}$)	9.7 (1)	27 (1)	35	170	21	–
Eu(III) ($\times10^{-7}$)	1.2 (1)	2.8 (1)	1.1	2.9 (Gd(III))	0.48	2.1 (Gd(III))

[a] Ref. [34], [b] Ref. [46], [c] Ref. [41], [d] Ref. [39]

Dissociation kinetics

The kinetic inertness of lanthanide complexes represents a key requisite for their *in vivo* applications since the products of the dissociation reactions, both free Ln^{3+} ions and ligands, are toxic for living systems. The dissociation of LnDOTA-like complexes is very slow and generally proceeds through a proton-assisted pathway without the involvement of endogenous metal ions like Zn(II) and Cu(II).[33, 34, 47, 48] To obtain information about the kinetic inertness of the Gd(III) complexes, the dissociation reactions of Gd**L1** and Gd**L2** were investigated in the presence of a large excess of H^+ ([HCl]=0.05 – 1.0 M) in order to ensure the occurrence of pseudo-first order conditions. These reactions were monitored by ^{1}H-NMR relaxometry at 20 MHz and 298 K. The relaxivity values of Gd**L1** and Gd**L2** in 0.95 M HCl as a function of time are shown in Figure S7. Considering the relatively high protonation constant of the aminoethyl group in Gd**L1** and Gd**L2** ($\log K_{GdHL}$=9.24 and 8.40, respectively; Table 2), the dissociation reactions is very likely to proceed *via* decomplexation of the monoprotonated Gd(HL) complexes. The proposed mechanism for the dissociation of Gd**L1** and Gd**L2** is shown in Scheme 3, whereas the definitions and equations used for the evaluation of the kinetic data are reported in the Supporting Information.

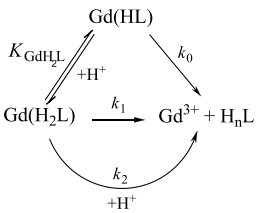

Scheme 3. Proposed reaction pathways for the dissociation of the protonated complexes Gd(H**L1**) and Gd(H**L2**).

In Table 4, the rate constants and the protonation constants characterizing the dissociation reactions of Gd(H**L1**) and Gd(H**L2**) are compared with the corresponding values for GdDOTA and GdDO3A. The half-lives ($t_{1/2}$) of dissociation of Gd(III) complexes calculated at pH=7.4 are also reported.

The values of the k_0 rate constant describing the spontaneous dissociation of Gd(H**L1**) and Gd(H**L2**) are extremely low and characterized by large errors, to indicate the irrelevance of the spontaneous dissociation for the monoprotonated complexes. The k_1 and k_2 values, the proton assisted dissociation rate constants, differ considerably between the Gd(III) complexes of **L1** and **L2**. The k_1 value of Gd(H**L1**) is comparable with that of GdDOTA and 4 orders of magnitude smaller than that of GdDO3A, due to the particularly strong coordination of the amide oxygen atom. On the other hand, Gd(H**L2**) shows a k_1 value almost three order of magnitude higher than that of Gd(HL**1**), being thus significantly more labile than Gd(H**L1**) and GdDOTA. Nevertheless, Gd(H**L2**) is significantly more inert than GdDO3A due to the coordination of the propionamide pendant arm. It is worth to make a comparison of k_1 values of Gd(H**L2**) with Ce(DO3A-*N*prop),[46] since DO3A-*N*prop ligand contain a propionate pendant arm and thus, like in Gd(H**L2**), it forms a six-membered chelate ring upon lanthanide ion coordination. Hence, since the k_1 values are almost comparable, it can be assumed that the interaction between the Ln^{3+} ion and the amide or the carboxylate oxygen atom of propionate pendant arms are very similar. The proton assisted dissociation of Gd(H**L1**) and Gd(H**L2**) proceeds through the protonation of the complexes at a carboxylate group. However, the resulting protonated complex is not reactive, since the protonation/deprotonation step of a carboxylate group is fast and the COO^- group can coordinate again. Thus, dissociation is more likely to occur by proton transfer from the carboxylic acid to the N-atom of the ring, resulting in a relatively labile protonated intermediate. In such intermediate, the proton displaces the Gd^{3+} ion from the coordination cage, thereby causing the dissociation of the GdL complex. The protonation constants (K^H_{GdH2L}) of Gd(H**L1**) and Gd(H**L2**) (Table 4) are relatively small and comparable to the K^H_{GdHL} value of GdDOTA,[34] which indicates that the protonation is likely to take place at the carboxylate group. Finally, the $t_{1/2}$ values of Gd(H**L1**) and Gd(H**L2**) are an additional proof that the kinetic inertness of both Gd(III)-complexes is superior than that of GdDO3A (Table 4). In conclusions, these data suggest that both Ln**L1** and Ln**L2** could represent good platforms for the development of LnDOTA-like bioconjugate systems for molecular imaging applications.

Table 4. Rate and equilibrium constants and half-lives ($t_{1/2}=\ln2/k_d$, pH=7.4) for the dissociation reactions of Gd(H**L1**), Gd(H**L2**) GdDO3A and GdDOTA complexes (298 K).

	Gd(H**L1**)	Gd(H**L2**)	Ce(**DO3A-***N***prop**)[a]	Gd(**DOTA**)[b]	Gd(**DO3A**)[d]
I	1.0 M KCl	1.0 M KCl	0.1 M KCl	0.15 M NaCl	0.1 M KCl
k_0 **(s^{-1})**	–	–	–	6.74×10^{-11}	–
k_1 **($M^{-1}s^{-1}$)**	$(2.6\pm0.2)\times10^{-6}$	$(2.1\pm0.2)\times10^{-3}$	7×10^{-3}	1.83×10^{-6}	2.3×10^{-2}
k_2 **($M^{-1}s^{-1}$)**	$(3.1\pm0.4)\times10^{-5}$	$(3.5\pm0.3)\times10^{-2}$	0.51	–	–
K^H_{GdHL}	1.7×10^9 (pH-pot)	2.5×10^8 (pH-pot)	260	14[c]	115[e]
$K^H_{GdH_2L}$	3.1 ± 0.5	15 ± 3	0.74	–	–
k_d **(s^{-1}) pH=7.4**	1.0×10^{-13}	8.4×10^{-11}	2.8×10^{-10}	7.3×10^{-14}	9.2×10^{-10}
$t_{1/2}$ **(h) pH=7.4**	1.9×10^9	2.3×10^6	6.9×10^5	2.6×10^9	2.1×10^5

[a] Ref. [46], [b] Ref. [47], [c] Ref. [34], [d] Ref. [30], [e] Ref. [39]

Synthesis of GdDOTAMAP-cholic acid (L5)

To be able to interact strongly with macromolecular substrates thus achieving high relaxivities, a GdDOTAMAP-like chelate needs to be designed with a suitable targeting moiety linked to the coordination cage by a short spacer as little flexible as

View Article Online
DOI: 10.1039/C4DT03939D

possible. For these reasons, we synthesized a novel DOTAMAP-based bifunctional chelator bearing a short spacer terminating with a free carboxylic acid (**2** in Scheme 4) that can be covalently bound to specific biological carriers bearing a functionalizable amino group. In our case the DOTAMAP moiety was linked to a bile acid, known to strongly bind to the plasma protein and so to increase the circulation lifetime of the probe.[26]

The synthesis of **L5** (Scheme 4) started by the formation of benzyl 2-(acrylamido)acetate via acylation with acriloyl chloride under Schotten–Baumann conditions in a biphasic mixture of dichloromethane and aqueous potassium carbonate. Then, the alkylation of tri-*tert*-butyl 1,4,7,10-tetraazacyclododecane-1,4,7-triacetate (DO3A(O*t*Bu)$_3$) was accomplished via Michael addition of benzyl 2-(acrylamido)acetate followed by Pd/C catalysed hydrogenation of the benzyl ester to get the bifunctional chelator **2**.

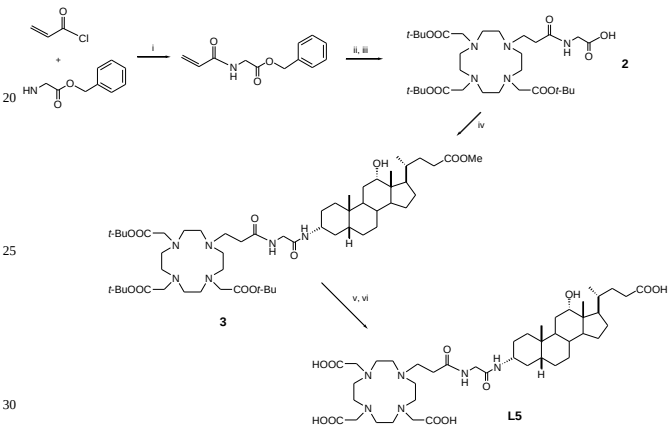

Scheme 4. Synthesis of DOTAMAP-cholic acid (**L5**): i) CH_2Cl_2, K_2CO_3/H_2O; ii) DO3A(tBu)$_3$, CH_3CN, *N*,*N*-diisopropylethylamine (DIPEA); iii) H_2, Pd/C, MeOH; iv) aminodeoxycholic acid ethyl ester, DMF, 1-[Bis(dimethylamino)methylene]-1*H*-1,2,3-triazolo[4,5-*b*]pyridinium 3-oxid hexafluorophosphate (HATU), DIPEA; v) LiOH, MeOH; vi) TFA, CH_2Cl_2.

The latter was reacted with (3β,5β,12α)-3-amino-12-hydroxycholan-24-oic acid methyl ester to obtain the fully protected ligand **3**. At this stage, the methyl ester was hydrolyzed using LiOH in MeOH and finally, the deprotected ligand **L5** was obtained as analytically pure white solids by precipitation with diethyl ether after hydrolysis of the *t*-butyl esters with TFA.

The Gd(III) complex was synthesized by adding small volumes of a stock solution of $GdCl_3$ to a solution of the ligand, maintaining the pH at 6.5 with diluted NaOH. The complexation process was monitored by measuring the change in the longitudinal water proton relaxation rate (R_1) at 20 MHz and 298 K (pH = 6.5) as a function of the concentration of Gd(III).

Relaxometric characterization and HSA interaction

The longitudinal relaxivity of Gd**L5** at 20 MHz and 310 K is 6.6 $mM^{-1}s^{-1}$, consistent with the presence of one metal bound water molecule and in agreement with the r_1 values measured under identical experimental conditions for related q=1 Gd-chelates of similar molecular weight. For instance, derivatives of GdDOTA and GdDTPA conjugated to cholic acid functionalities, such as a GdDTPA-cholic (r_1 = 6.4 $mM^{-1}\,s^{-1}$)[27] and a GdDOTA-cholic (r_1 ~ 5 $mM^{-1}s^{-1}$).[49] Only the recently reported Gd(III) complex with a deoxycholic acid derivative linked to the AAZTA chelator (AAZTA = 6-amino-6-methylperhydro-1,4-diazepine tetraacetic acid) resulted in a higher r_1 value as a result of the presence of two inner-sphere water molecules.[27]

Detailed information about the molecular parameters determining the relaxometric behaviour of Gd(III) complexes can be gained by recording and analysing the Nuclear Magnetic Relaxation Dispersion (^{1}H NMRD) profiles. This magnetic field dependence of the ^{1}H r_1 was measured, at 298 and 310 K, in the frequency range 0.01-70 MHz, corresponding to magnetic field strengths varying between 2.34×10^{-4} and 1.64 T (Figure 2). The profiles show the typical shape for low molecular weight complexes, with a region of constant r_1 at low fields, a dispersion around 2-5 MHz and another plateau at higher frequencies (> 10 MHz). The lower values of the relaxivity at 310 K over the entire range of frequencies proton Larmor confirm that r_1 is not limited by the change of water, but rather by the fast rotational motion of the complex. The experimental data were then analysed by a least-square fitting procedure to the established theory for paramagnetic relaxation, using the well-known Solomon–Bloembergen–Morgan (SBM) equations and Freed's model for the inner- and outer-sphere contributions to the proton relaxivity, respectively.[1] Some of the parameters involved in the description of the magnetic field dependence of r_1 can be fixed to standard values, typical of GdDOTA-like chelates. In particular, the number of coordinated water molecules (q) was fixed to one; the distance of closest approach of the outer-sphere water molecules to Gd^{3+} was set to 4.0 Å; the relative diffusion coefficient (D) was fixed to 2.24×10^{-5} $cm^2\ s^{-1}$ (298 K) and to the Gd–water proton distance (r_{Gd-H}) was attributed the value of 3.0 Å. In addition, for the exchange lifetime we used the same value previously determined for Gd**L2**, *i.e.*, $^{298}\tau_M$ = 12 ns. We then used Δ^2, τ_V, and τ_R as adjustable parameters and obtained the results reported in Table 5. The rotational correlation time τ_R is more than two times longer than for Gd**L2** and this simply reflect the increased molecular weight (slower tumbling) of the cholic acid derivative. The parameters associated with the electronic relaxation, Δ^2 and τ_V, assume values quite comparable to those found for Gd**L2**, which is a further evidence of a strictly similar coordination cage.

Table 5. Best-fit parameters obtained by analysis of the ^{1}H NMRD profiles for Gd**L5** and for the Gd**L5**/HSA adduct compared to parent Gd**L2** chelate.[a]

Parameters	GdL5	GdL5-HSA	GdL2[b]	GdL1[b]
Δ^2 /×10^{19} s^{-2}	3.2 ± 0.1	0.8 ± 0.1	3.9	3.8
$^{298}\tau_V$ / ps	21.3 ± 0.4	54.4 ± 0.2	15	11
$^{298}k_{ex}$ /×10^6 s^{-1}	81.2[b]	81.2[b]	81.2	1.1
$^{298}\tau_{RG}$ / ns	0.20 ± 0.01	40 ± 5	0.079	0.079
$^{298}\tau_{RL}$ / ns	---	0.64 ± 0.02	---	---
r_{Gd-H} / Å	3.00*	3.00*	3.00*	3.00*
S^2	---	0.37 ± 0.01	---	---

[a] For the parameters q, a and ^{298}D the values of 1, 4.0 Å, 2.24×10^{-5} $cm^2\ s^{-1}$, respectively, were used. [b] Ref. [19]. * Values fixed during the fitting

View Article Online
DOI: 10.1039/C4DT03939D

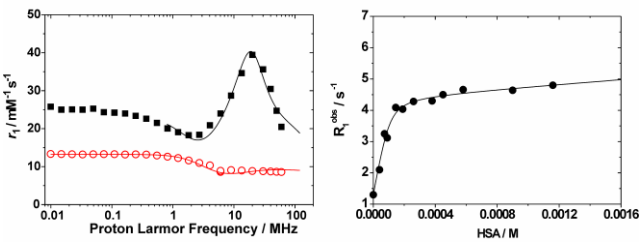

Figure 2. Left: ^{1}H NMRD profiles of Gd**L5** (empty circles) and of Gd**L5**/HSA adduct in the presence of 10 fold excess of HSA (filled squares) at 298 K. Right: water proton relaxation rate of a 0.1 mM aqueous solution of Gd**L5** as a function of HSA concentration (20 MHz, 298 K).

As mentioned above, deoxycholic acid is known to form host-guest adducts with HSA with high association constants. Since HSA is a protein of 66.437 Da, its reversible interaction with a functionalized Gd complex induces an increase of the reorientational correlation time τ_R of the paramagnetic system and hence marked relaxivity enhancements. The formation of the adduct between Gd**L5** and HSA was investigated through the well-established ^{1}H proton relaxation enhancement (PRE) technique. This consists in measuring the variation in the longitudinal relaxation rate, R_1, of a dilute solution of the paramagnetic guest for increasing concentrations of the host. With this method, the binding parameters K_A, n (the number of equivalent and independent binding sites), and r_1^b (the relaxivity of the resulting supramolecular adducts) can be assessed. To this end, a 0.1 mM solution of Gd**L5** was titrated with HSA, at 20 MHz and 298 K, and the least-squares fit of plot of R_1 versus HSA concentration (Fig. 2, right) enabled us to calculate the affinity constant [$K_A = (7.8 \pm 0.1) \times 10^4$ M^{-1}] and the relaxivity of the adduct ($r_1^b = 38.7 \pm 0.1$ mM^{-1} s^{-1}). This r_1 value is 4.4 times higher than that measured for the isolated complex and clearly reflects the slowing down of molecular tumbling as indicated by the presence in the ^{1}H NMRD profile of a narrow peak centred around 30 MHz (Figure 2). However, unlike many of the cases reported in the literature, the slowing down of rotational motion results in a large increase of r_1 because the limiting effect of the slow water exchange does not occur. This is the main advantage of the propionamide group: apart from minor effects on the thermodynamic stability, the leveling effect of the long τ_M is lifted and high relaxivity values can be attained. Similarly, a large relaxation enhancement has been recently observed by M. F. Ferreira *et al*. for the binding to HSA of the Gd(III) complex with the related DO3A-N-(α-pyrenebutanamido)propionate chelator.[22] Moreover, we observe that the r_1 value surpasses those reported for other HSA-bound Gd(III) complexes with $q = 1$ and bearing a cholic acid residue.[27, 49] In particular, a recent work has shown that the GdAAZTA-cholic acid system decreases its hydration state (from 2 to 1) upon interaction with the protein and the r_1 of the host-guest adduct is only 29.0 mM^{-1}s^{-1} (20 MHz, 298 K). In the same report, an r_1 value of 26.8 mM^{-1}s^{-1} was measured for a $q = 1$ GdDTPA-like chelate bearing the same cholic acid residue, under analogous experimental conditions. The analysis of the NMRD profile requires the use of the model-free Lipari-Szabo approach incorporated into the SBM equations for the *IS* relaxation mechanism.[50, 51] This model allows to take into account the contribution of a faster local motion (τ_{RL}) of the coordination cage about the binding group superimposed to the overall global rotation of the paramagnetic supramolecular adduct (τ_{RG}). The correlation of the two types of motions is described by the parameter S^2 whose value may vary between zero (completely independent motions) and one (totally correlated motions). The best-fit parameters, reported in Table 5, indicate a relatively restricted degree of internal rotation of Gd**L5** about the deoxycholic group at the binding site. At the same, it is clear that at the imaging fields (1.5 – 3 T) the relaxivity is dominated by the local rotational dynamics (τ_{RL} and S^2) rather than by the exchange of the bound water molecule.

Conclusions

The introduction of an additional methylene group into an acetamide arm in DOTA-monoamide derivatives has a pronounced impact on the water exchange dynamics of the corresponding, neutral Gd(III) complexes. The value of kex increases by ca. two orders of magnitude and this implies that the limiting effect on the relaxivity by a slow rate of water exchange is removed when GdDOTAMAP chelates are conjugated to macromolecules or nanosized scaffolds. This is further demonstrated by the new cholic acid GdDOTAMAP derivative that shows a high affinity for HSA, giving rise to a supramolecular adduct whose relaxivity, 38.7 mM^{-1} s^{-1} at 20 MHz and 298 K, is in the upper range of values for $q = 1$ Gd-chelates. The thermodynamic and kinetic data in aqueous solution outline that the replacement of an acetamide arm with a propionamide moiety only results in a negligible decrease of logK_{GdL} ($1<\Delta\log K<2$). From the point of view of the kinetic inertness, the effects are more pronounced, as shown by the $t_{1/2}$ values for the dissociation of GdL that decreases by three order of magnitude passing from the acetamide (Gd**L1**) to the propionamide (Gd**L2**) coordination. Nevertheless, Gd**L2** is significantly more inert than established Gd-chelates such as GdDTPA oe GdDO3A.
In general, neutral macrocyclic complexes of lanthanide(III) cations present several advantages as imaging probes in preclinical studies. GdDOTAMAP appears particularly interesting as MRI contrast agent since it combines favourable properties in terms of stability and inertness with the occurrence of a fast exchange regime for the bound water molecule that allows the achievement of large relaxivity enhancements.

Experimental

All chemicals were purchased from Sigma-Aldrich or Alfa Aesar unless otherwise stated and were used without further purification. Ligands **L1** and **L2** were synthesized as reported in the literature.[19,52] ^{1}H and ^{13}C NMR spectra were recorded on Bruker Avance III spectrometer operating at 11.74 T. Chemical shifts are reported relative to TMS and were referenced using the residual proton solvent resonances. Electrospray ionization mass spectra (ESI MS) were recorded on a SQD 3100 Mass Detector (Waters), operating in positive or negative ion mode, with 1% v/v formic acid in methanol as the carrier solvent.

Synthesis of Benzyl 2-(acrylamido)acetate. A solution of acryloyl chloride (300 µL; 3.67 mmol) in dry CH_2Cl_2 (5 mL) was slowly added at 0°C to a suspension of benzyl glycinate (1,03 g;

View Article Online
DOI: 10.1039/C4DT03939D

6,23 mmol) and K_2CO_3 (1,5 g; 11.01 mmol) in dry CH_2Cl_2 (15 mL) under N_2 atmosphere. The reaction mixture was stirred for 1 h at RT and then evaporated *in vacuo*. The resulting oil was dissolved in CH_2Cl_2 (10 mL), washed with HCl 0.1 M (5 mL) and H_2O for three times and dried with Na_2SO_4. The organic solution was then filtered and evaporated under reduced pressure to obtain the product (439 mg, 2.00 mmol, yield 55%). ^{1}H NMR (400 MHz, $CDCl_3$): 4.14 (s, 2H, NH*CH*$_2$CO), 5.18 (s, 2H, *CH*$_2$ benzyl); 5,64 - 5.67 (m, 2H, *CH*$_2$=CH); 6.11 – 6.37 (m, 1H, CH_2=*CH*); 7.33 – 7.35 (m, 5H, *CH* phenyl) ppm. ^{13}C NMR (400 MHz, $CDCl_3$): 41.53 (NH*C*H$_2$CO), 67.38 (*C*H$_2$ benzyl); 127.41 (*C*H$_2$=CH); 128.27 (*C*H phenyl); 130.19 (CH_2=*CH*); 135.18 (C phenyl), 165.71 (*C*ONHCH$_2$) 169.98 (*C*OOBn) ppm. ESI-MS$^+$ calculated for $C_{12}H_{14}NO_3$ [M+H]$^+$: 220,24; found: 220.12.

Synthesis of DOTAMAP-Gly-Bn (1): A solution of DO3A(*t*Bu)$_3$ (0.1 g; 0.19 mmol), DIPEA (99 µL; 0.57 mmol) and benzyl 2-(acrylamido)acetate (83 mg; 0.38 mmol) in CH_3CN (5 mL) was refluxed overnight. The crude product was purified by silica gel chromatography (95:5 DCM/methanol) to afford **3** (55 mg, 0.076 mmol, yield 40%). ^{1}H NMR (400 MHz, $CDCl_3$): 1.42 (s, 27H, C*H*$_3$); 2.66-2.74 (m, 2H, NC*H*$_2$CH$_2$CO); 3.05-3.26 (m, 16H, C*H*$_2$ ring); 3.28-3.30 (m, 2H, NCH$_2$C*H*$_2$CO); 3.36 (s, 6H, NC*H*$_2$CO); 4.66 (s, 2H, NHC*H*$_2$CO), 5.23 (s, 2H, C*H*$_2$ benzyl); 7.25 – 7.34 (m, 5H, C*H* phenyl) ppm. ^{13}C NMR (400 MHz, $CDCl_3$): 28.25 (C(*C*H$_3$)$_3$); 29.75 (N*C*H$_2$CH$_2$CO); 43.31 (NH*C*H$_2$CO); 48.31 (N*C*H$_2$CH$_2$CO); 52.10-52.21 (*C*H$_2$ ring); 61,2 (N*C*H$_2$CO); 65.23 (*C*H$_2$ benzyl); 81.24 (*C*(CH$_3$)$_3$); 127.76 (*C*H phenyl); 141.18 (*C* phenyl), 166.98 (*C*ONHCH$_2$); 170.88 (*C*OOBn); 171,2 (*C*OC(CH$_3$)$_3$) ppm. ESI-MS$^+$ calculated for $C_{38}H_{64}N_5O_9$ [M+H]$^+$: 734.93; found: 735.04.

Synthesis of DOTAMAP-Gly (2): Pd/C (10% w/w, 73 mg) was added to the solution of **1** (730 mg, 1 mmol) in MeOH (15 mL) and the reaction was stirred under H_2 for 2 days at RT. Then, the solution was filtered on celite and dried under reduced pressure to obtain **2** (643 mg, 1 mmol, quantitative yield). ^{1}H NMR (400 MHz, $CDCl_3$): 1.38 (s, 27H, C(C*H*$_3$)$_3$); 2.70-2.73 (m, 2H, NCH$_2$C*H*$_2$CO); 3.01-3.35 (m, 16H, C*H*$_2$ ring); 3.31-3.36 (m, 2H, NCH$_2$C*H*$_2$CO); 3.43 (s, 6H, NC*H*$_2$CO); 4.71 (s, 2H, NHC*H*$_2$COOH) ppm. ^{13}C NMR (400 MHz, $CDCl_3$): 28.38 (C(*C*H$_3$)$_3$); 31.41 (NCH$_2$*C*H$_2$CO); 45.21 (NH*C*H$_2$CO); 49.02 (N*C*H$_2$CH$_2$CO); 52.01-52.74 (*C*H$_2$ ring); 60,1 (N*C*H$_2$CO); 81.75 (*C*(CH$_3$)$_3$); 166.98 (*C*ONHCH$_2$); 170,8 (*C*OC(CH$_3$)$_3$); 173.25 (*C*OOH). ESI-MS$^+$ calculated for $C_{31}H_{58}N_5O_9$ [M+H]$^+$: 644,81; found: 645.12.

Synthesis of DOTAMAP-Gly-cholic acid methyl ester (3). Compound **2** (302 mg, 0.47 mmol) was dissolved in DMF (20 mL), then HATU (535 mg, 1.41 mmol) and DIPEA (163 µL, 0.94 mmol) were added. Then, (3β,5β,12α)-3-Amino-12-hydroxycholan-24-oic acid methyl ester (198 mg, 0.47 mmol) dissolved in DMF (3 mL) was added. The reaction was attired at RT overnight. The mixture was evaporated *in vacuo* and the crude product was washed with H_2O (3 x 5 mL) and then purified by silica gel chromatography (95:5 CH_2Cl_2/MeOH) to afford **3** (162 mg, 0.16 mmol, yield 33%). ^{13}C NMR (400 MHz, $CDCl_3$): 12.76 (*C*H$_3$), 17.36 (*C*H$_3$), 23.58 (*C*H$_2$), 23.90 (*C*H$_3$), 25.87 (*C*H$_2$), 26.68 (*C*H$_2$), 27.41 (*C*H$_2$), 28.10 (C(*C*H$_3$)$_3$), 28.90 (*C*H$_2$), 29.09 (*C*H$_2$), 29.31 (*C*H$_2$), 30.90 (*C*H$_2$), 31.06 (*C*H$_2$), 32.90 (NCH$_2$*C*H$_2$CO), 33.12 (*C*H), 34.62 (*C*CH$_3$), 35.07 (*C*H$_2$), 35.84 (*C*H), 36.58 (*C*H), 37.65 (*C*H), 44.98 (*C*H), 46.00 (NH*C*H$_2$CO); 46.54 (*C*H), 46.83 (*C*CH$_3$), 48.30 (*C*HNH), 49.17 (N*C*H$_2$CH$_2$CO), 52.0-53.1 (*C*H$_2$ ring), 61.80 (N*C*H$_2$CO*t*Bu), 74.65 (*C*HOH), 81.91 (*C*(CH$_3$)$_3$), 164.78 (*C*ONHCH$_2$), 167.41 (*C*ONH), 169.50 (*C*OC(CH$_3$)$_3$) ppm. ESI-MS$^+$ calculated for $C_{56}H_{99}N_6O_{12}$ [M+H]$^+$: 1048,41; found: 1048.50.

Synthesis of DOTAMAP-gly-cholic acid (L5). the protected ligand **3** (160 mg, 0.15 mmol) was reacted overnight at RT with LiOH (10.8 mg, 0.45 mmol) in THF (5 mL). The solution was then dried under reduced pressure and the product was dissolved in CH_2Cl_2 and washed thrice with H_2O (5 mL). The organic solution was then dried with Na_2SO_4, filtered and evaporated under reduced pressure to obtain the intermediate that was further reacted by dissolving it in DCM:TFA (1:1 v/v 2mL : 2mL). The mixture was stirred overnight at RT. After evaporation *in vacuo*, Et_2O was added and the precipitate formed was washed twice with Et_2O to obtain the ligand **L5** as hydrated trifluoacetate salt (150 mg, 0.134 mmol, 90% yield).^{13}C NMR (400 MHz, D_2O): 12.66 (*C*H$_3$), 16.87 (*C*H$_3$), 23.43 (*C*H$_2$), 23.95 (*C*H$_3$), 24.20 (*C*H$_2$), 25.33 (*C*H$_2$), 26.12 (*C*H$_2$), 28.75 (*C*H$_2$), 29.13 (*C*H$_2$), 30.16 (*C*H$_2$), 30.96 (*C*H$_2$), 31.15 (*C*H$_2$), 32.90 (NCH$_2$*C*H$_2$CO), 33.18 (*C*H), 34.38 (*C*CH$_3$), 35.53 (*C*H$_2$), 35.94 (*C*H), 37.68 (*C*H), 41.51 (*C*H), 46.46 (NH*C*H$_2$CO), 46.71 (CH), 48.10 (*C*H), 49.03 (*C*CH$_3$), 49.14 (*C*HNH), 49.95 (N*C*H$_2$CH$_2$CO), 50.0-53.0 (*C*H$_2$ ring), 60.22 (NCH$_2$COOH), 73.19 (*C*HOH), 170.13 (*C*ONH), 172.30 (*C*ONHCH$_2$), 173.49 (*C*OOH), 178.80 (*C*OOH, deoxycholic acid) ppm. ESI-MS$^+$ calculated for $C_{43}H_{73}N_6O_{12}$ [M+H]$^+$: 866,06; found: 866.20. CHN: calculated for $C_{43}H_{72}N_6O_{12}\cdot 2CF_3COOH\cdot 3H_2O$: C, 49.90; H, 7.13; N, 7.43; found: C, 48.96; H, 7.35; N, 7.78.

Equilibrium measurements: The chemicals used for the experiments were of analytical grade. The $LnCl_3$ solutions were prepared from $LnCl_3\cdot xH_2O$ (x=5-7) (*Aldrich*; 99.9%). The concentration of the $LnCl_3$ solutions were determined by complexometric titration with standardized Na_2H_2edta and *xylenol orange* as indicator. The concentration and the protonation constants of H_3**L1** and H_3**L2** was determined by pH-potentiometric titration in the presence and absence of a large (40-fold) excess of $CaCl_2$ ([L]=0.002 M). The pH-potentiometric titrations were made with standardized 0.2 M KOH. The stability constants of the Ln(III)-complexes with **L1** and **L2** were determined using the "out-of-cell" technique because of the slow formation reactions. The pH range and the time needed to reach the equilibria were determined by spectrophotometry for the formation of Ce**L1** and Ce**L2** (the UV absorption band of the Ce(III) resulting from the 4f – 5d transition is very sensitive for complex formation). Eight samples for each Ln(III) complexes of **L1** and **L2** were prepared in the range of 2.5 - 4.0 ([Ln^{3+}]=[L]=0.002 M). The samples were kept at 298 K for 12 weeks to reach the equilibrium. For the calculations of the stability constants of the Ln**L1** and Ln**L2**, the protonation constants of the Ln(III)-complexes were also used, which were

View Article Online
DOI: 10.1039/C4DT03939D

calculated from the pH-potentiometric titration curve of the Ln**L1** and Ln**L2** complexes in the pH range of 1.7 – 11.7. For the pH measurements and titration, a *Metrohm 785 DMP Titrino* titration workstation and a *Metrohm-6.0233.100* combined electrode were used. Equilibrium measurements were carried out at a constant ionic strength (0.1M KCl) in 6 mL samples at 298 K. The solutions were stirred and N_2 was bubbled into them. The titrations were made in the pH range of 1.7-11.7. For the calibration of the pH meter, KH-phthalate (pH=4.005) and borax (pH=9.177) buffers were used. For the calculation of $[H^+]$ from the measured pH values, the method proposed by *Irving et al.* was used.[53] A 0.01M HCl solution was titrated with the standardized KOH solution in the presence of 0.1 M KCl ionic strength. The differences between the measured (pH_{read}) and calculated pH ($-\log[H^+]$) values were used to obtain the equilibrium H^+ concentration from the pH values, measured in the titration experiments. The ionic product of water was found to be $\log K_w$=13.85, which was calculated from the pH potentiomtric data of 0.01M HCl solution titrated with the standardized KOH solution at 25°C in 0.1 M KCl in the pH range 10.5 – 11.7. The stability constant of Ce**L1** was determined by spectrophotometry looking at the absorption bands of Ce(III)-complexes in the wavelength range of 220-345 nm. Eight samples of Ce^{3+}-**L1** were prepared in the range of 2.5 - 4.2 ($[Ce^{3+}]=[L]=0.0015$ M). The pH of the sample were adjusted by stepwise addition of a solution of KOH and HCl . The ionic strength of solutions was maintained by 0.1 M KCl. The samples were kept at 298 K for 12 weeks. The absorbance values of the samples were determined at 10 wavelengths (304, 308, 312, 316, 320, 324, 328, 332, 336 és 340 nm) on the absorption band of Ce(H**L1**). For the calculations of the stability constants of the Ce**L1**, the molar absorbancies of the Ce^{3+} and Ce(H**L1**) were determined by recording the spectra of 1.0×10^{-3}, 2.0×10^{-3} and 3×10^{-3} M solutions of Ce^{3+} and Ce(H**L1**) (pH=6.0, 0.1 M KCl, 25 °C). The protonation constant of the Ce**L1** was also determined by pH-potentiometric titrations of Ce**L1** in the pH range of 1.7 – 11.7 ([Ce**L1**]=0.002 M). The spectrophotometric experiments were performed with Cary 1E spectrophotometer and 1 cm quartz cuvette at 298 K. The protonation and stability constants were calculated with the PSEQUAD program.[54]

Kinetic studies: Formation rates of Ce(III)- and Eu(III)-complexes of **L1** and **L2** were determined by spectrophotometry at 320 and 255 nm, respectively, and in the pH range about 3.7 - 6.0. The concentration of the ligands was 2×10^{-4} M. The formation of Ln(III)-complexes was studied in the presence of a 5 to 50 fold Ln^{3+} excess in order to keep the pseudo-first-order conditions. The pseudo-first-order rate constants (k_{obs}) were calculated by fitting the absorbance values to the Eqn. (5):

$$A_t = (A_0 - A_e)e^{(-k_{obs}t)} + A_e \qquad (5)$$

where A_0, A_e and A_t are the absorbance values at the start, at equilibrium and at the time t of the reaction. The temperature was maintained at 298 K and the ionic strength of the solutions was kept constant (0.1 M KCl). In order to keep the pH values constant, 1,4-dimethylpiperazine (pH range 3.2 - 4.1), *N*-methylpiperazine (pH range 4.1 - 5.2) and piperazine (pH range 4.7 - 6.6) buffers (0.01 M) were used.

The kinetic inertness of Gd**L1** and Gd**L2** was characterized by the rates of the dissociation reactions taking place in 0.05 – 1.0 M [HCl] solution. The dissociation reactions of GdL1 and GdL2 were followed by measuring the longitudinal relaxation time of H_2O protons (T_1) with a *Bruker MQ20 Minispec* spectrometer at 20 MHz. The temperature of the sample holder was controlled with a thermostated air stream. The longitudinal relaxation time was measured with the "inversion recovery" method (180° - τ - 90°) by using 8 different τ values. The measurements were performed with 1 mM solution of the GdL1 and GdL2 complexes, so the relaxation rate values were given as $r_1=1/T_{1p} + 1/T_{1w}$ where T_{1p} and T_{1w} were the relaxation time of water protons in the presence and absence of Gd(III) complexes. The pseudo-first-order rate constants (k_d) were calculated by fitting the relaxation rate ($1/T_{1p}$) data to Eqn. (6).

$$r_t = (r_r - r_v)e^{(-k_d t)} + r_v \qquad (6)$$

where r_r, r_t and r_v are the relaxivity values of reactants (Gd(HL1): r_{1p}= 4.6 $mM^{-1}s^{-1}$, Gd(HL2): r_{1p}= 4.9 $mM^{-1}s^{-1}$, 20 MHz, 25°C),[19] the product (Gd^{3+}: r_{1p}= 13.1 $mM^{-1}s^{-1}$, 20 MHz, 25 °C) and at the time t of the reaction. The temperature was maintained at 298 K and the ionic strength of the solutions was kept constant ([HCl]+[KCl]=1.0 M). The calculation of the kinetic parameters were performed by the fitting of the absorbance - time and relaxation rate – time data pairs with the *Micromath Scientist* computer program (version 2.0, Salt Lake City, UT, USA).[55]

Relaxometric measurements: The water proton longitudinal relaxation rates as a function of the magnetic field strength were measured in non-deuterated aqueous solutions on a fast field-cycling Stelar SmarTracer relaxometer (Stelar s.r.l., Mede (PV), Italy) over a continuum of magnetic field strengths from 0.00024 to 0.25 T (corresponding to 0.01-10 MHz proton Larmor frequencies). The relaxometer operates under computer control with an absolute uncertainty in $1/T_1$ of ± 1%. Additional longitudinal relaxation data in the range 15-70 MHz were obtained on a Stelar Relaxometer connected to a Bruker WP80 NMR electromagnet adapted to variable-field measurements (15-80 MHz proton Larmor frequency). The exact concentration of Gd^{III} was determined by measurement of bulk magnetic susceptibility shifts of a *t*BuOH signal or by inductively coupled plasma mass spectrometry (ICP-MS, Element-2, Thermo-Finnigan, Rodano (MI), Italy). The ^1H T_1 relaxation times were acquired by the standard inversion recovery method with typical 90° pulse width of 3.5 μs, 16 experiments of 4 scans. The temperature was controlled with a Stelar VTC-91 airflow heater equipped with a calibrated copper–constantan thermocouple (uncertainty of ±0.1 °C).The non-covalent interaction of GdL5 with HSA was evaluated by using the Proton Relaxation Enhancement (PRE) method: R_1 was monitored as a function of

View Article Online
DOI: 10.1039/C4DT03939D

the amount of HSA added to 0.1 mM Gd**L5** solution, at 298 K and 20 MHz, while maintaining the pH at 6-7.

Acknowledgements

This research was supported in part by the European Union and the State of Hungary, co-financed by the European Social Fund in the framework of TÁMOP 4.2.4. A/2-11-1-2012-0001 'National Excellence Program' (grant no.: A2-MZPD-12-0038) (Zs. B). The research was also supported by the EU and co-financed by the European Social Fund under the project TÁMOP 4.2.2.A-11/1/KONV-2012-0043 (V.A.). Z. B. and A.V. also thank the Hungarian Scientific Research Found (OTKA K109029). The Italy-Hungary Intergovernmental S&T Cooperation Program (HU11MO2-TET_10-1-2011-0202) is also gratefully acknowledged.

Notes and references

[a] *Dipartimento di Scienze ed Innovazione Tecnologica, Università del Piemonte Orientale "Amedeo Avogadro", Viale T. Michel 11, I-15121, Alessandria, Italy. E-mail: mauro.botta@mfn.unipmn.it*
[b] *Department of Inorganic and Analytical Chemistry, University of Debrecen, H-4010, Debrecen, Egyetem tér 1., Hungary.*

†Electronic Supplementary Information (ESI) available: UV-spectrophotometric studies of Ce^{3+}-**L1** system, species distribution of Gd^{3+}-**L1** and Gd^{3+}-**L2** systems, formation kinetics of Ln(H**L1**) and Ln(H**L2**), dissociation kinetics of Gd**L1** and Gd**L2**, ^{1}H NMRD profile of Gd**L5** at 310 K. See DOI: 10.1039/b000000x/

References

1. P. Caravan, J. J. Ellison, T. J. McMurry and R. B. Lauffer, *Chem. Rev.*, 1999, **99**, 2293-2352.
2. E. Brücher, G. Tircsó, Z. Baranyai, Z. Kovács and A. D. Sherry, in *The Chemistry of Contrast Agents in Medical Magnetic Resonance Imaging*, eds. A. S. Merbach, L. Helm and E. Toth, John Wiley & Sons, Ltd, 2nd Edition edn., 2013, pp. 157-208.
3. T. Grobner, *Nephrol., Dial., Transplant.*, 2006, **21**, 1104-1108.
4. P. Marckmann, L. Skov, K. Rossen, A. Dupont, M. B. Damholt, J. G. Heaf and H. S. Thomsen, *J. Am. Soc. Nephrol.*, 2006, **17**, 2359-2362.
5. K. Kitajima, T. Maeda, S. Watanabe, Y. Ueno and K. Sugimura, *Int. J. Urol.*, 2012, **19**, 1127-1127.
6. L. Telgmann, C. Wehe, J. Künnemeyer, A.-C. Bülter, M. Sperling and U. Karst, *Anal. Bioanal. Chem.*, 2012, **404**, 2133-2141.
7. T. Frenzel, P. Lengsfeld, H. Schirmer, J. Hutter and H. J. Weinmann, *Invest. Radiol.*, 2008, **43**, 817-828.
8. H. Pietsch, P. Lengseld, T. Steger-Hartmann, A. Lowe, T. Frenzel, J. Huetter and M. A. Sieber, *Invest. Radiol.*, 2009, **44**, 226-233.
9. N. Fretellier, J.-M. Idée, A. Dencausse, O. Karroum, S. Guerret, N. Poveda, G. Jestin, C. Factor, I. Raynal, P. Zamia, M. Port and C. Corot, *Invest. Radiol.*, 2011, **46**, 292-300.
10. G. W. White, W. A. Gibby and M. F. Tweedle, *Invest. Radiol.*, 2006, **41**, 272-278.
11. S. Aime, P. L. Anelli, M. Botta, F. Fedeli, M. Grandi, P. Paoli and F. Uggeri, *Inorg. Chem.*, 1992, **31**, 2422-2428.
12. L. Lattuada, A. Barge, G. Cravotto, G. B. Giovenzana and L. Tei, *Chem. Soc. Rev.*, 2011, **40**, 3019-3049.
13. P. L. Anelli, L. Calabi, C. De Haën, F. Fedeli, P. Losi, M. Murru and F. Uggeri, *Gazz. Chim. It.*, 1996, **126**, 89 - 97.
14. D. A. Keire and M. Kobayashi, *Bioconjugate Chem.*, 1999, **10**, 454-463.
15. E. Boros, M. Polasek, Z. Zhang and P. Caravan, *J. Am. Chem. Soc.*, 2012, **134**, 19858-19868.
16. B. N. Siriwardena-Mahanama and M. J. Allen, *Dalton. Trans.*, 2013, **42**, 6724-6727.
17. S. Aime, M. Botta, M. Fasano, S. G. Crich and E. Terreno, *J. Biol. Inorg. Chem.* , 1996, **1**, 312-319.
18. M. Botta and L. Tei, *Eur. J. Inorg. Chem.*, 2012, 1945-1960.
19. L. Tei, G. Gugliotta, Z. Baranyai and M. Botta, *Dalton Trans.*, 2009, 9712-9714.
20. Z. Jászberényi, A. Sour, É. Tóth, M. Benmelouka and A. E. Merbach, *Dalton Trans.*, 2005, 2713-2719.
21. M. F. Ferreira, A. F. Martins, J. A. Martins, P. M. Ferreira, É. Tóth and C. F. G. C. Geraldes, *Chem Commun*, 2009, 6475-6477.
22. M. F. Ferreira, G. Pereira, A. F. Martins, C. I. O. Martins, M. I. M. Prata, S. Petoud, É. Tóth, P. M. T. Ferreira, J. A. Martins and C. F. G. C. Geraldes, *Dalton Trans.*, 2014, **43**, 3162-3173.
23. M. F. Ferreira, A. F. Martins, C. I. O. Martins, P. M. Ferreira, É. Tóth, T. B. Rodrigues, D. Calle, S. Cerdan, P. Lopez-Larrubia, J. A. Martins and C. F. G. C. Geraldes, *Contrast Media & Mol. Imaging*, 2013, **8**, 40-49.
24. A. D. Sherry, R. D. Brown, C. F. G. Geraldes, S. H. Koenig, K. T. Kuan and M. Spiller, *Inorg. Chem.*, 1989, **28**, 620-622.
25. F. A. Rojas-Quijano, G. Tircsó, E. T. Benyó, Z. Baranyai, H. T. Hoang, F. K. Kálmán, P. K. Gulaka, V. D. Kodibagkar, S. Aime, Z. Kovács and A. D. Sherry, *Chem. - Eur. J.*, 2012, **18**, 9669-9676.
26. P. L. Anelli, L. Lattuada, V. Lorusso, G. Lux, A. Morisetti, P. Morosini, M. Serleti and F. Uggeri, *J. Med. Chem.*, 2004, **47**, 3629-3641.
27. E. Gianolio, C. Cabella, S. Colombo Serra, G. Valbusa, F. Arena, A. Maiocchi, L. Miragoli, F. Tedoldi, F. Uggeri, M. Visigalli, P. Bardini and S. Aime, *J. Biol. Inorg. Chem.* , 2014, **19**, 715-726.
28. V. Lorusso, L. Pascolo, C. Fernetti, M. Visigalli, P. Anelli and C. Tiribelli, *Biochem. Biophys. Res. Commun.*, 2002, **293**, 100-105.
29. J. F. Desreux, E. Merciny and M. F. Loncin, *Inorg. Chem.*, 1981, **20**, 987-991.
30. A. Takács, R. Napolitano, M. Purgel, A. C. Bényei, L. Zékány, E. Brücher, I. Tóth, Z. Baranyai and S. Aime, *Inorg. Chem.*, 2014, **53**, 2858-2872.
31. A. Bianchi, L. Calabi, C. Giorgi, P. Losi, P. Mariani, P. Paoli, P. Rossi, B. Valtancoli and M. Virtuani, *J. Chem. Soc., Dalton Trans.*, 2000, 697-705.
32. H. Sigel, B. Prijs and R. B. Martin, *Inorg. Chim. Acta*, 1981, **56**, 45-49.
33. É. Tóth, R. Király, J. Platzek, B. Radüchel and E. Brücher, *Inorg. Chim. Acta*, 1996, **249**, 191-199.
34. É. Tóth, E. Brücher, I. Lázár and I. Tóth, *Inorg. Chem.*, 1994, **33**, 4070-4076.
35. S. L. Wu and W. D. Horrocks, *Inorg. Chem.*, 1995, **34**, 3724-3732.
36. J. Moreau, E. Guillon, J. C. Pierrard, J. Rimbault, M. Port and M. Aplincourt, *Chem. - Eur. J.*, 2004, **10**, 5218-5232.
37. E. Brücher, G. Laurenczy and Z. S. Makra, *Inorg Chim Acta*, 1987, **139**, 141-142.
38. X. Wang, T. Jin, V. Comblin, A. Lopez-Mut, E. Merciny and J. F. Desreux, *Inorg. Chem.*, 1992, **31**, 1095-1099.

View Article Online
DOI: 10.1039/C4DT03939D

39. K. Kumar and M. F. Tweedle, *Inorg. Chem.*, 1993, **32**, 4193-4199.
40. L. Burai, I. Fábián, R. Király, E. Szilágyi and E. Brücher, *J. Chem. Soc., Dalton Trans.*, 1998, 243-248.
41. E. Szilágyi, É. Tóth, Z. Kovács, J. Platzek, B. Radüchel and E. Brücher, *Inorg. Chim. Acta*, 2000, **298**, 226-234.
42. Z. Baranyai, G. A. Rolla, R. Negri, A. Forgács, G. B. Giovenzana and L. Tei, *Chem. - Eur. J.*, 2014, **20**, 2933-2944.
43. K. Kumar, C. A. Chang and M. F. Tweedle, *Inorg. Chem.*, 1993, **32**, 587-593.
44. W. P. Cacheris, S. K. Nickle and A. D. Sherry, *Inorg. Chem.*, 1987, **26**, 958-960.
45. K. Kumar, C. A. Chang, L. C. Francesconi, D. D. Dischino, M. F. Malley, J. Z. Gougoutas and M. F. Tweedle, *Inorg. Chem.*, 1994, **33**, 3567-3575.
46. E. Balogh, R. Tripier, P. Fouskova, F. Reviriego, H. Handel and É. Tóth, *Dalton Trans.*, 2007, 3572-3581.
47. Z. Baranyai, Z. Pálinkás, F. Uggeri, A. Maiocchi, S. Aime and E. Brücher, *Chem. - Eur. J.*, 2012, **18**, 16426-16435.
48. P. Wedeking, K. Kumar and M. F. Tweedle, *Magn. Reson. Imaging*, 1992, **10**, 641-648.
49. P. Verwilst, S. V. Eliseeva, S. Carron, L. V. Elst, C. Burtea, G. Dehaen, S. Laurent, K. Binnemans, R. N. Muller, T. N. Parac-Vogt and W. M. De Borggraeve, *Eur. J. Inorg. Chem.*, 2011, 3577-3585.
50. G. Lipari and A. Szabó, *J. Am. Chem. Soc.*, 1982, **104**, 4546-4559.
51. G. Lipari and A. Szabó, *J. Am. Chem. Soc.*, 1982, **104**, 4559-4570.
52. A. Barge, L. Tei, D. Upadhyaya, F. Fedeli, L. Beltrami, R. Stefania, S. Aime and G. Cravotto, *Org. Biomol. Chem.*, 2008, **6**, 1176-1184.
53. H. M. Irving, M. G. Miles and L. D. Pettit, *Anal. Chim. Acta*, 1967, **38**, 475-488.
54. Zékány L and Nagypál I, in *Computational Methods for the Determination of Formation Constants*, ed. Leget DJ, Plenum Press, New York, 1985, pp. 291 - 353.
55. *Micromath Scientist*, (1995) MicroMath Inc, Salt Lake City, UT, USA.

View Article Online
DOI: 10.1039/C4DT03939D

Table of contents entry

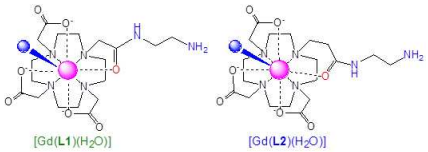

$\log K_{GdL}$	22.25 (4)	20.22 (3)
Dissociation half-life $t_{½}$ (h) (pH 7.4)	1.9×10^{9}	2.3×10^{6}
Formation rate of EuL k_{OH} (s^{-1})	1.2×10^{7}	2.8×10^{7}
Water exchange rate k_{ex} ($\times 10^{6}$ s^{-1})	1.1	81.2
r_1 ($mM^{-1}s^{-1}$)	4.6	4.9

GdDOTA propionamide derivatives preserve a good thermodynamic stability and kinetic inertness while possessing a rate of water exchange two orders of magnitude greater than GdDOTA acetamide.